UNITED NATIONS EDUCATIONAL, SCIENTIFIC AND CULTURAL ORGANIZATION
INTERNATIONAL CENTRE FOR THEORETICAL PHYSICS
I.C.T.P., P.O. BOX 586, 34100 TRIESTE, ITALY, CABLE: CENTRATOM TRIESTE

H4.SMR/773-21

College on Medical Physics:
Radiation Protection and Imaging Techniques

5 - 23 September 1994

MRI Spectroscopy

J. Pirš

University of Ljubljana
Department of Physics
Ljubljana, Slovenia

College on Medical Physics:
Radiation Protection and Imaging Techniques

15 - 23 September 1994

NMR IN SPECTROSCOPY

J. Pirš, M. Eržen, B. Marin
+G. Gomišček, E. Moser

Jožef Stefan Institute
Ljubljana, Slovenia

+Institut für Medizinishe Physik
Universitaet Wien, Austria

MRI SPECTROSCOPY

MRI SPECTROSCOPY

J.Pirš, V.Eržen, B.Marin - Jožef Stefan Institute, Ljubljana

G.Gomišček, E.Moser - Institut fur Medizinische Physik, Wien

INTRODUCTION

Nuclear magnetic resonance imaging (MRI) is developing into a powerful tool in medical ciagnostics. In order to produce the state of the art, medically useful images (Figure 1.), this technique has evolved into sophisticated and complex technology, that should in spite of this fact, be well understood by the medical personnel. Figure 2. shows a picture of a professional MR Imaging System. It is of course financially unacceptable to use such an instrumentation for teaching and demonstration purposes. As a consequence, demonstration of MRI which illustrates the essential features of NMR techniques, is of utmost necessity. The Institute Jozef Stefan NMR Spectrometer/Imager is the first demonstration instrument of this kind.

It was developed as the result of the joint efforts and experiences of Jožef Stefan Institute, Ljubljana, SLO, Institute fur Medizinische Physik Wien, Austria and Waterloo NMR Spectrometers Inc., Waterloo, Canada.

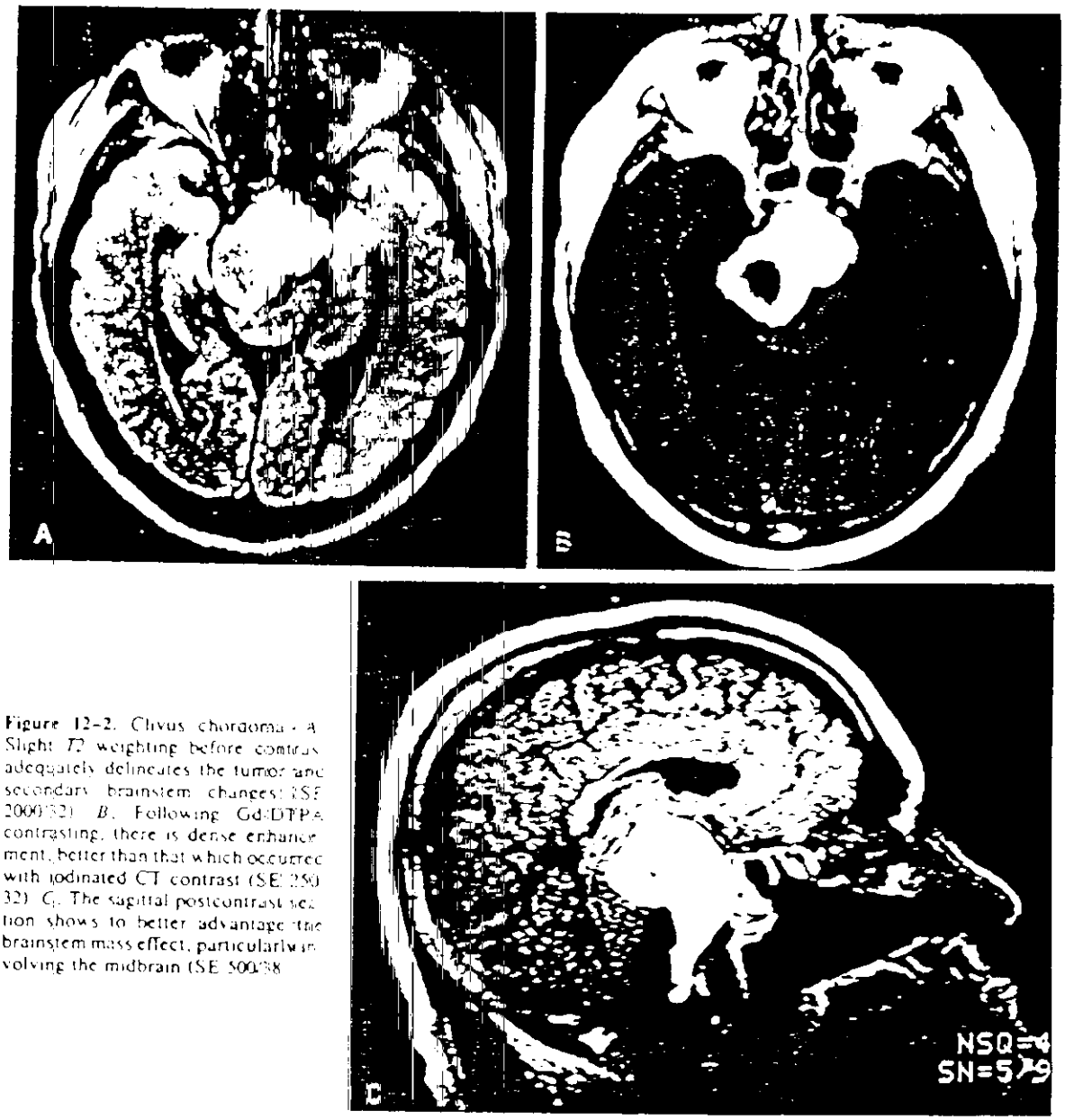

Figure 12-2. Clivus chordoma. *A*, Slight *T2* weighting before contrast adequately delineates the tumor and secondary brainstem changes (SE 2000/32). *B*, Following Gd-DTPA contrasting, there is dense enhancement, better than that which occurred with iodinated CT contrast (SE 250/32). *C*, The sagittal postcontrast section shows to better advantage the brainstem mass effect, particularly involving the midbrain (SE 500/38).

Figure 1.

TOMIKON BMT 1100

The MR imaging system TOMIKON BMT 1100 uses a resistive magnet with integrated iron shielding developed and patented by BRUKER. The maximum magnetic field strength is 0.28 Tesla. This system meets all the requirements for routine and research-oriented clinical proton imaging:

- **Trouble-free installation**

  [illegible] stray magnetic field
  [illegible] many siting restrictions
  reasonable weight and floor loading
  compact dimensions, minimal room requirements
  easy integration into existing buildings

- **Simple operation**

  menu based software
  routine protocols called from a keypad
  A minimum of easily understood controls

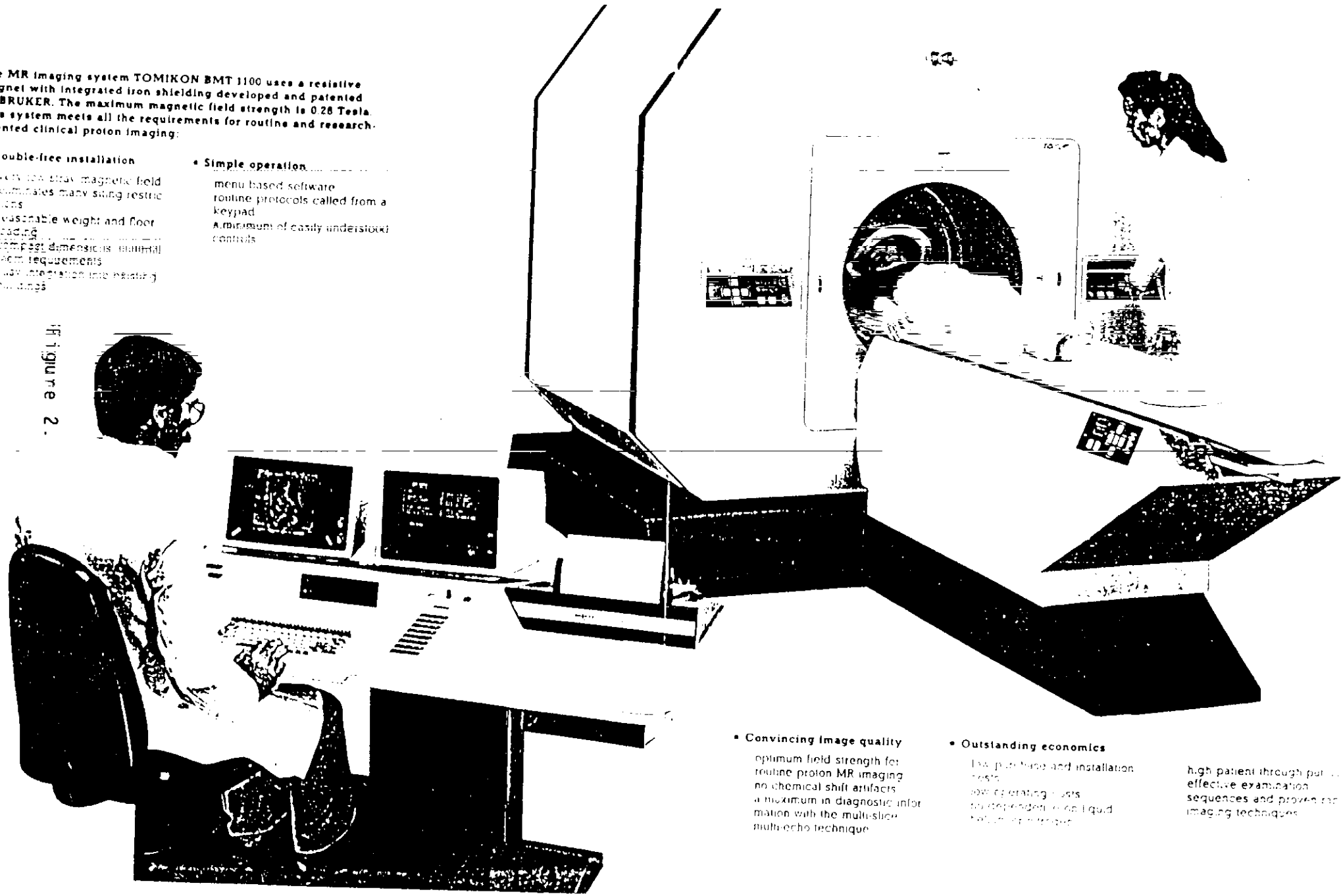

- **Convincing image quality**

  optimum field strength for routine proton MR imaging
  no chemical shift artifacts
  a maximum in diagnostic information with the multi-slice multi-echo technique

- **Outstanding economics**

  [illegible] purchase and installation costs
  [illegible] operating costs
  [illegible] independent of liquid [illegible]

high patient through-put ... effective examination sequences and proven ... imaging techniques

Figure 2.

SMALL MR IMAGER AND NMR SPECTROMETER (SMRI)

The instrument is ideall for undergraduate and graduate physics and medical physics laboratories. The special emphasis is given to the demonstration of MR imaging of phantom samples that can give an adequate understanding of NMR techniques without occupying expensive professional MR imaging instruments in hospitals for demonstration and teaching purposes. It can however allow for the demonstration of all other essential effects of NMR as well:

- free induction decay
- spin-echo
- spin-spin and spin-lattice relaxation
- self-diffusion of molecules
- FFT of the free induction decay
- NMR tomography

The Small MR Imager and NMR Spectrometer consists of two units:

- Pulsed NMR Spectrometer MS4
- Digital data acquisition & processing system LCD SCOPE

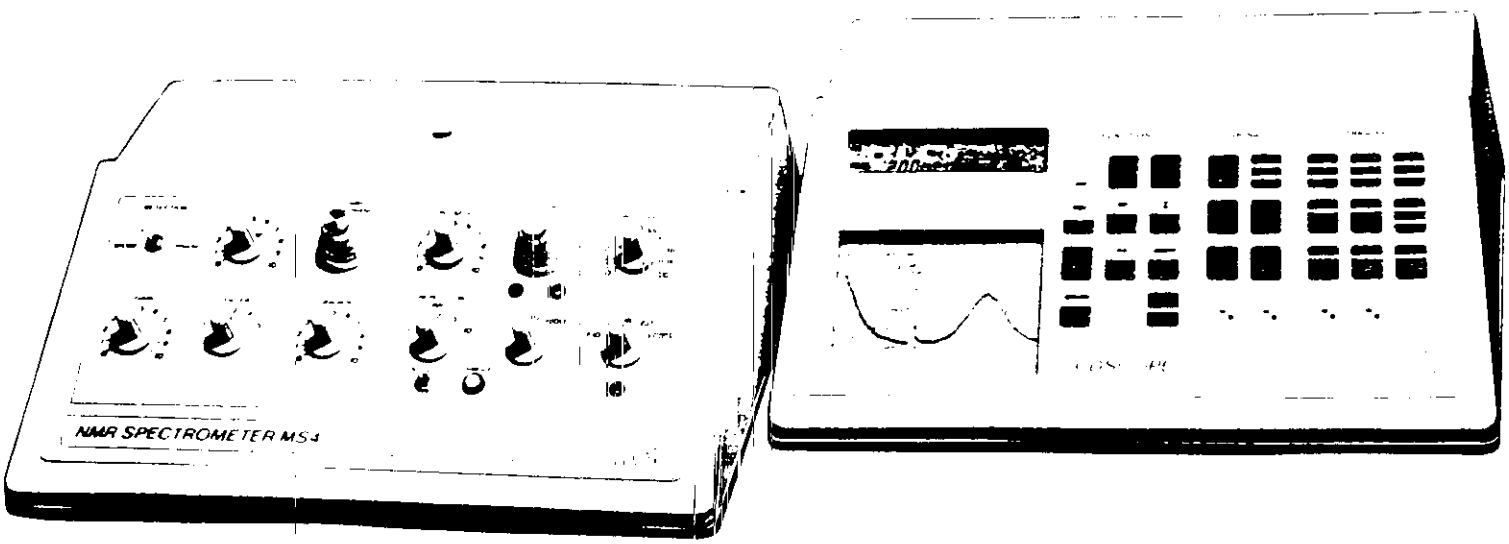

Figure 3. - Small MR Imager and NMR Spectrometer

The NMR spectrometer MS4 is a self contained fixed frequency spectrometer. It allows for the application and demonstration of all standard techniques (free precession, spin-echo, inversion-recovery, Carr Purcell, NMR tomography). The built in permanent magnet provides a stable, homogeneous magnetic field. In order to allow for the MR imaging, the magnet has a built-in gradient coil system, that can generate a linear gradient of the z-component of the magnetic field ($\partial B_z/\partial z$). The digital data acquisition and processing system (LCD SCOPE) has all the performances of the digital oscilloscope. The system microcomputer controls the operation of the entire measuring system and performs all necessary calculations (signal amplitude, digital averaging, integral, Fourier transform,...). It can also provide interfacing the external IBM PC XT/AT computer. The external IBM PC computer is in principle not necessary as long as one wants to perform the basic NMR experiments. However in the case of the MR Imaging experiment the external computer is unavoidable as it performs the image reconstruction. The available communication & data processing software guides the user through the entire set of basic NMR experiments providing all necessary information, performs MR image reconstruction and also allows for large screen live projection of the NMR experiments using the digital overhead projector (See fig.1. and Table I).

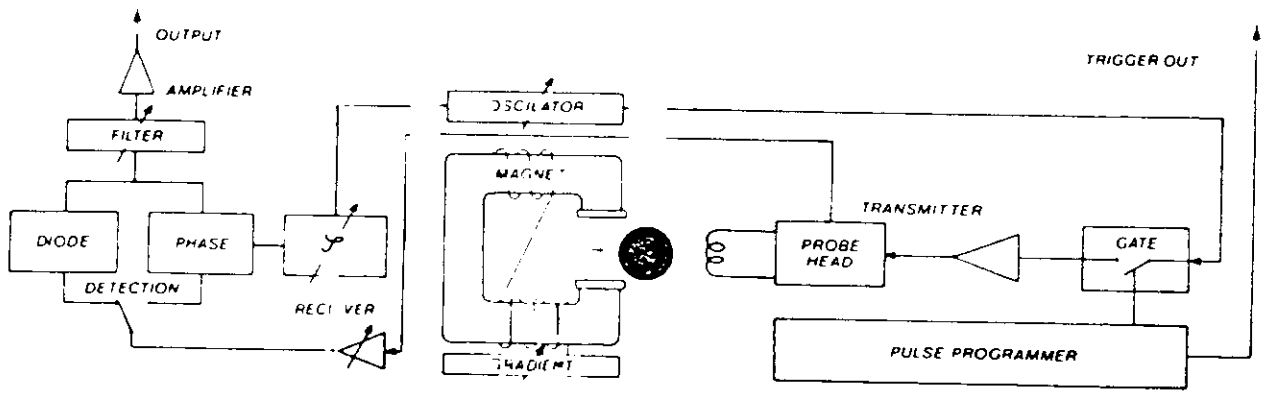

Figure 4. - NMR spectrometer MS4 - Block diagram

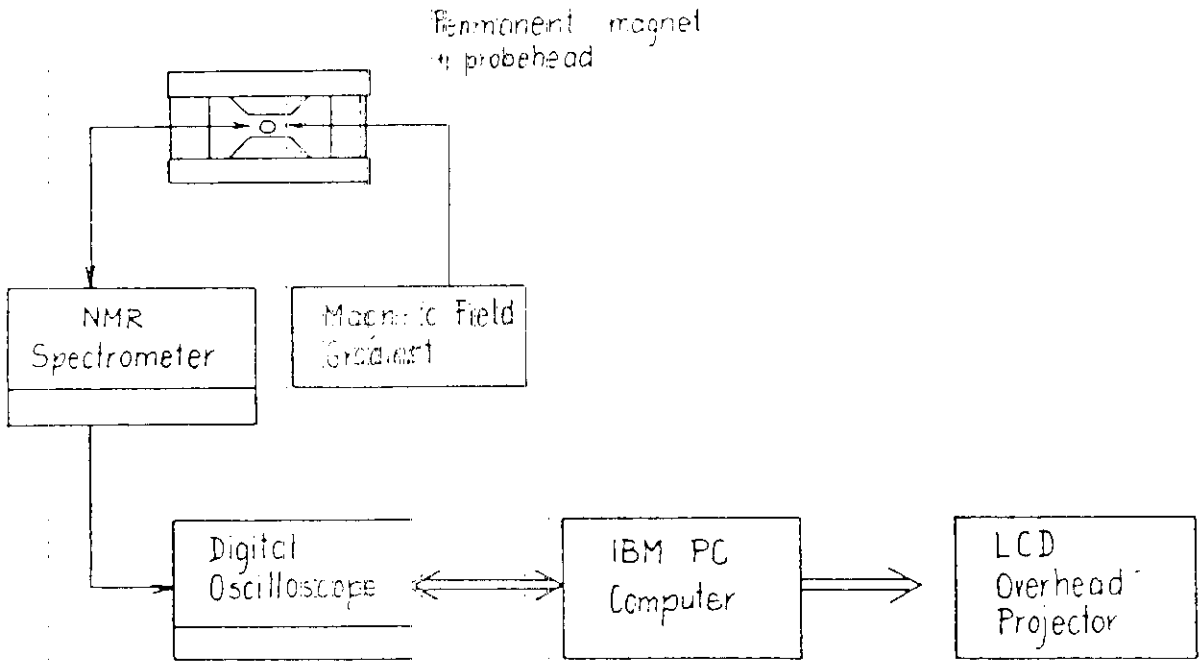

Small MR Imager and NMR Spectrometer
Block diagram

Figure 5.

SPECIFICATIONS

Frequency	9 MHz
Magnetic field: strength	0.21 T
homogeneity	10^{-6} T/cm
Magnetic field gradient	0 to $2^{1} \times 10^{-4}$ T/cm
Sample dimensions	outer diameter 8 mm, length 10 mm
Pulse sequences	$\pi/2$; $\pi/2 - t - \pi$ Hahn echo; $\pi - t - \pi/2$ inversion recovery; Carr-Purcell sequence
R.f. phase channels	0°, 90° phase shifted with respect to the reference
R.f. transmitter power	$\pi/2$ r.f. pulse is about 10^{-3} T
Receiver recovery time	$\pm$ 100 us
Detection	phase sensitive and diode
Signal to noise	$\geq$ 100
Gain variation	two orders of magnitude
Sampling frequency	variable in steps 1-2-5-10 from 2 MHz to 0.04 Hz
A/D resolution	0.5 %
Data memory	512 or 2048 bytes
Display	LCD matrix 200 x 120
External computer interface	RS 232 C

IBM PC XT/AT compatible

IBM PC communication and data processing software

Table I.

BASIC NMR EXPERIMENTS

The SMRI instrument is designed to measure the nuclear magnetic resonance observables such as free induction decay (FID), spin-echo, spin-spin and spin relaxation times, self-diffusion coefficient and in the first place, MR images of phantom objects.

When the sample containing protons is inserted into the NMR coil in the center of the built-in permanent magnet, the nuclear magnetization orients along the static magnetic field. If an intense radiofrequency field at a resonant frequency:

$$\omega_L = \gamma B_o$$

where ω = Larmor frequency
γ = gyromagnetic ratio
B_o = static magnetic field

the nuclear magnetization starts nutating away from the axis of the static magnetic field (z-axis). If the length of the r.f. pulse is properly adjusted, the magnetization will end up perpendicular to the static magnetic field (90^0 pulse). Being perpendicular to the magnetic field it will precess around the magnetic field axis at a Larmor frequency nducing a signal in the NMR coil -free precession signal. Due to the local inhomogeneities of the magnetic field caused by field gradient and spin-spin interactions the partial local magnetizations will precess with different Larmor frequencies. So partial magnetization will soon get dephased and the signal will decay to zero (See Fig. 6).

The entire process can be very well followed by the SMRI instrument that allows for the adjustment of the resonance condition, the 90^0 pulse length, the detector gain and the detector reference phase. Throughout the entire experiment the free precession signal is followed by the digital oscilloscope and displayed on its LCD matrix screen.

FREE PRECESSION SIGNAL

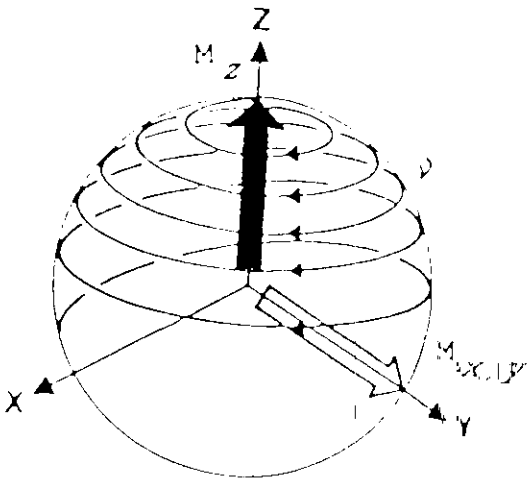

Rotation of the magnetisation under the effect of the r.f. pulse

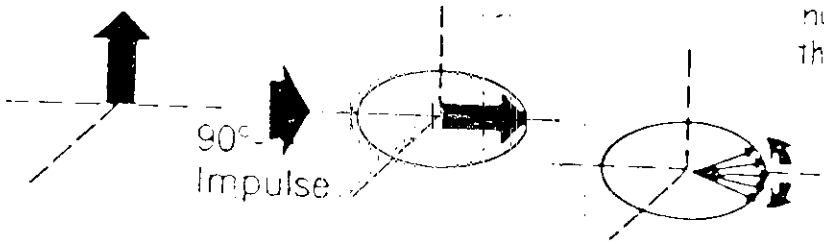

Time dependence of the nuclear magnetisation in the rotating frame

FID

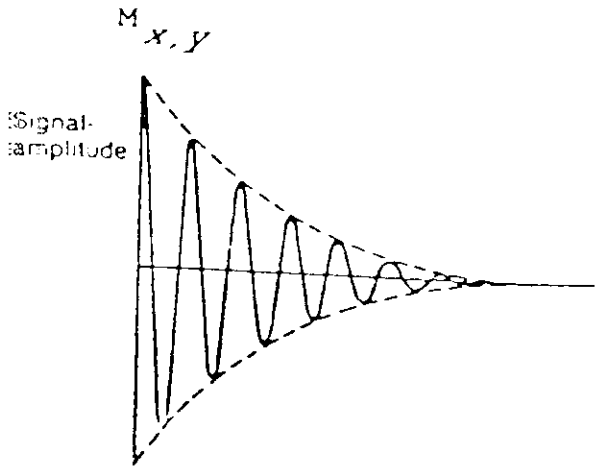

Figure 6.

If the static inhomogeneity of the magnet is the major reason for a decay of the free precession signal, the second r.f. pulse, being twice as long as the first 90^0 pulse - 180^0 pulse, will cause a time reversal in the relative motion of partial magnetizations. So the partial magnetization that got dephased during the time between the first r.f. pulse and the second r.f. pulse (180^0) will refocus again after the same time that elapsed between the first and the second r.f. pulse. The signal called the spin-echo will appear (See Fig. 7). The refocusing of the spins would be complete (spin-echo signal = FID) if there were no spin-spin interactions. As these interactions are time dependent a time reversal" caused by a 180^0 pulse cannot correct for the partial magnetization dephasing due to spin-spin interactions. Therefore the amplitude of the spin-echo will decay with increasing delay time t between the first and the second pulse with the characteristic time called spin-spin relaxation time T^2 (See Fig. 8). So repeating this experiment for a number of times with different delay times t, one can get the spin-spin relaxation time T^2 from the dependence of the spin-echo amplitude of the delay times t.

Instead of measuring the time dependence of the spin-echo amplitude by varying the delay time t between 90^0 and 180^0 pulse, one can apply another 180^0 pulse after the time t after the first spin-echo signal. This pulse will again cause refocusing of the magnetization and appearance of another spin-echo signal. Repeating this procedure for number of times one gets the well known Carr - Purcell pulse sequence. This sequence generates a train of spin-echo signals. Just as in the case of the single spin-echo experiment the amplitudes of the spin-echo signals generated this way decay with the spin-spin relaxation time T_2 See Fig. 9). So using this sequence one can measure spin-spin relaxation time T_2 in one single experiment.

The decay of the nuclear free precession signal is not governed only by the magnetic field inhomogeneity and spin-spin interactions described abowe. As the FID signal is caused by the precession of the transverse magnetization generated by the 90^0 r.f. pulse one can expect that this magnetization will sooner or latter return to its equilibrium orientation along the static magnetic field.

SPIN ECHO

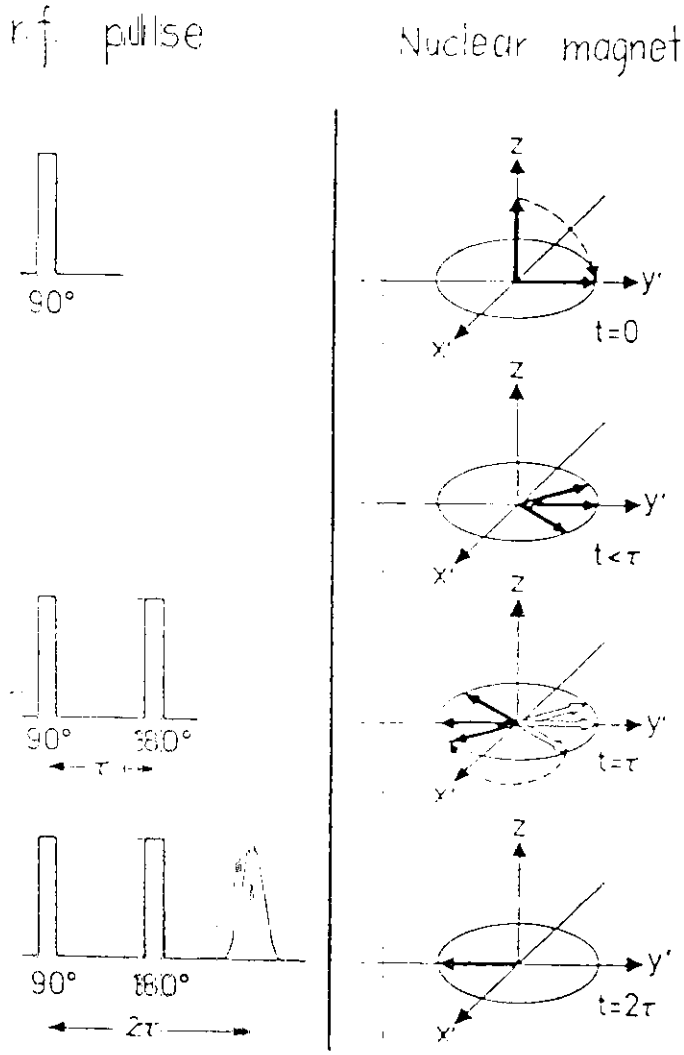

Time evolution of nuclear magnetisation during the Spin-echo pulse sequence

Figure 7.

SPIN SPIN RELAXATION TIME T_2

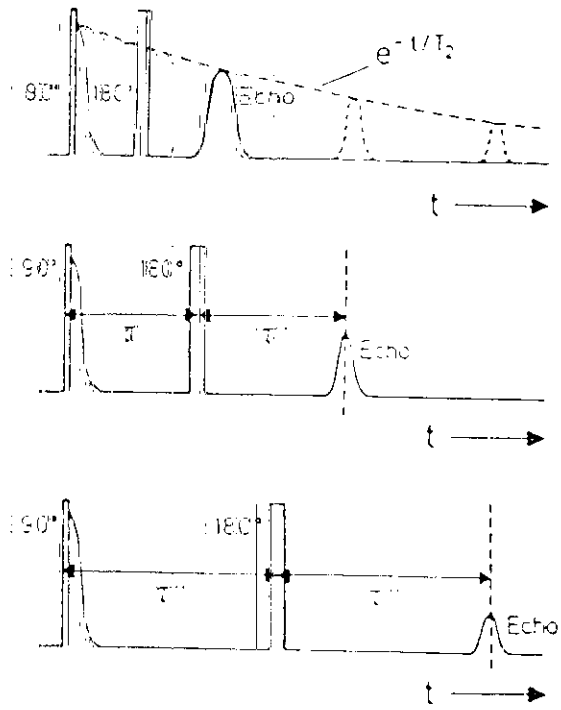

Time dependence of the spin echo amplitude

Figure 8.

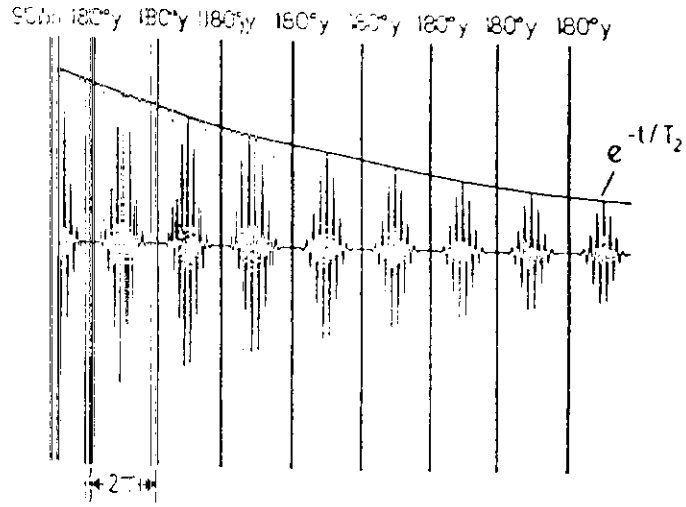

Carr - Purcell pulse sequence

Figure 9.

A simple thermodyramic analogy of relaxation of nuclear magnetization towards original rest state is based on the concept of spin temperature. Following r.f. excitation, the spins can be considered "hot". The environment, generally referred to as "lattice", (even in liquids) can be perceived as a heat sink with a large heat capacity, absorbing the nuclei's excess energy through thermal contact (Fig.10). However, the spins are actually quite effectively insulated from the lattice. Hence the "heat" transfer is slow, and relaxation times are consequently long. In pure water, the proton spin-lattice relaxation time at room temperature is approximately 3 seconds. In biological tissue, it varies between a few hundred milliseconds and about 2 seconds.

The experiments that determine the spin-lattice relaxation rate are based on the fact, that the signal following the 90^0 pulse is proportional to the magnetization **parallel** to the magnetic field.

If at the beginning of the experiment, that has to determine the spin-lattice relaxation time T_1, 180^0 pulse is applied to the sample, the magnetization is inverted to be antiparallel to the magnetic field. As such orientation is not thermodynamically stable, the magnetization will relax with the spin-lattice relaxation time towards the equilibrium orientation. After time t after the first 180^0 pulse a 90^0 pulse is applied. The signal following it is proportional to the magnetization component parallel to the magnetic field. Varying the delay time t between the 180^0 pulse and the 90^0 pulse one can determine the time evolution of the component of the magnetization parallel to the magnetic field by measurirg the amplitude of the free precession signal following the 90^0 pulse. This experiment is a well known **inversion recovery method.**

Inversion Recovery (180° - t - 90°)

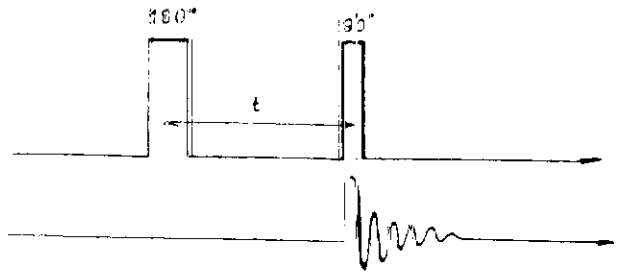

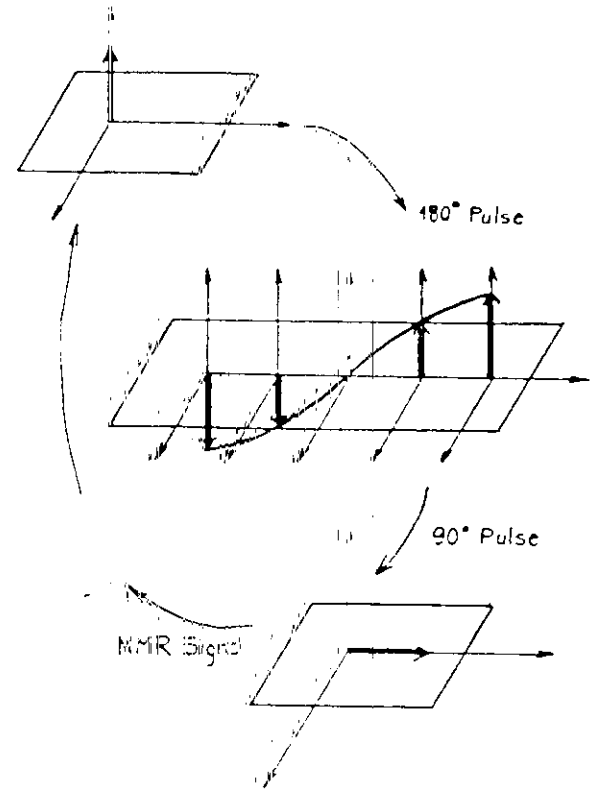

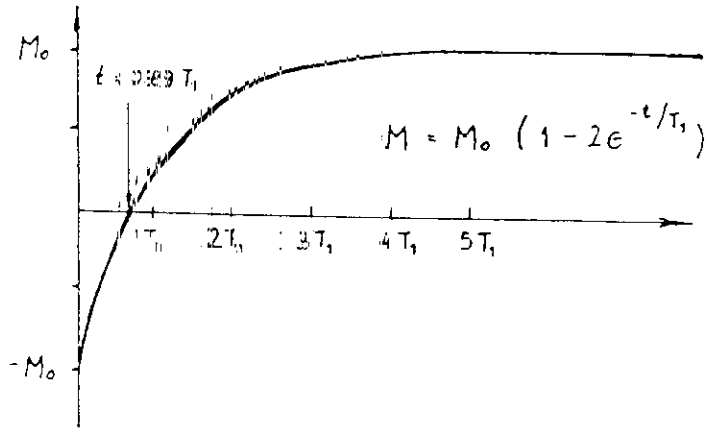

Time dependence of the FID signal following the 180° pulse

Figure 10. - Inversion recovery method

The basic principle of magnetic resonance imaging is the conversion of the spatial dependence of NMR parameters (spin density, spin lattice and spin-spin relaxation times) into the frequency dependence. As the Larmor precession frequency is proportional to the static magnetic field

the spatial variation of the magnetic field induces spatial variation of Larmor frecuency . The required variation of the magnetic field can be best done with set of gradient coils producing linear gradient of the z-component of the magnetic field. By making the nuclei "see' different static magnetic field values according to their spatial location, one can in principle, differentiate signals eritted from nuclei in different volume elements voxels. All NMR imaging methods are based on this fundamental principle (Fig.11).

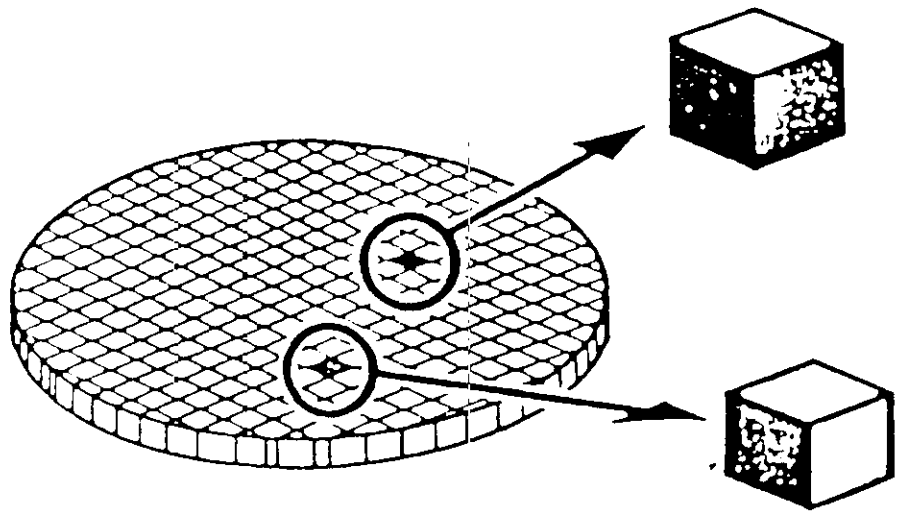

Two different volume elements (voxels) corresponding to different values of the detected magnetization.

Figure 11.

This can be illustrated with a simple phantom consisting of a teflon block having two water-filled cylindrical holes aligned with the z axis (axis of the static field), but with different locations with respect to x (Fig.12). In the absence of a gradient, (Gx=0) the samples are indistinguishable. They resonate at exactly the same frequency, because they experience the same field, and hence, the free induction decay contains only one frequency. (Fig.12a). However, as soon as the gradient is turned on, the two tubes will no longer experience the same magnetic field strength, and the resulting free induction decay will be the superposition of two different frequency components (Fig.12b).

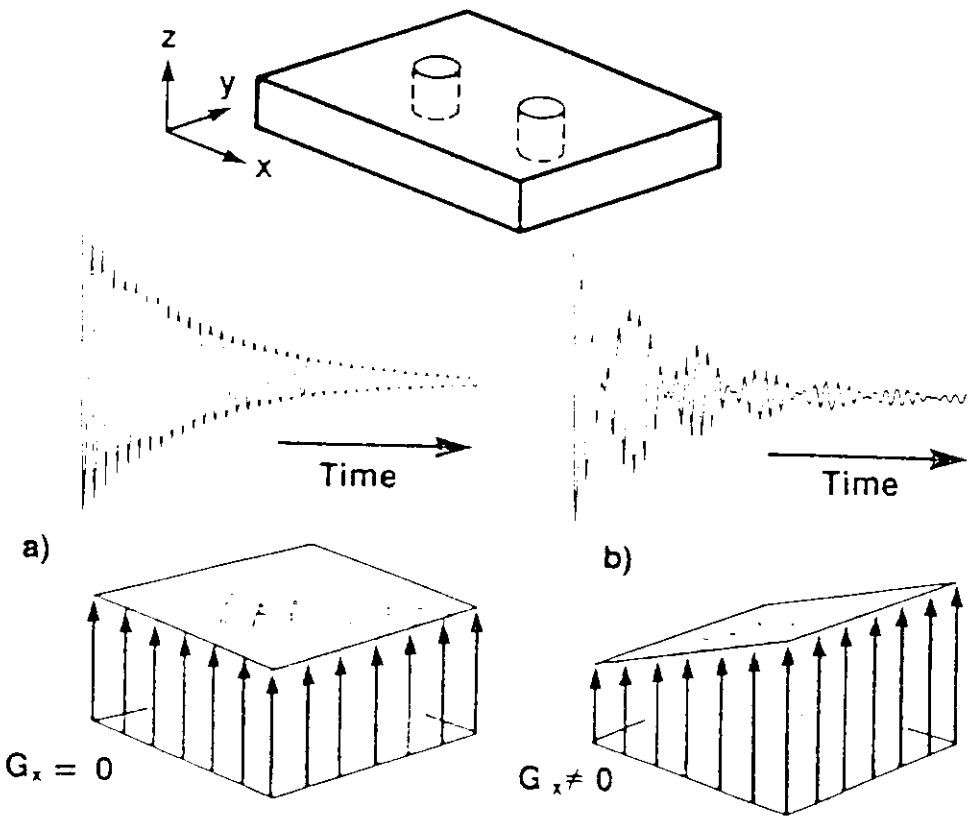

In the absence of the field gradient ($G_x = G_y = G_z = 0$) both samples sense the same field; the free induction decay therefore consists of a single frequency (Fig. a). In the presence of a gradient G_x, the two samples sense different fields, resulting in a free induction signal consisting of two frequencies (Fig. b).

Figure 12.

In reality, signals are collected from a multitude of spatial locations and the FID is a composite consisting of many different frequencies. To determine individual frequencies in such situations, one resorts to a mathematical analysis, carried out in a digital computer. The process is called Fourier transform. Whereas the FID represents the time evolution of the transverse magnetization, the Fourier transform represents its frequency distribution. This not only allows extraction of the individual frequencies, but also their associated amplitudes, which are proportional to the spin density at the particular spatial location. However, a Fourier transform of one orientation of such phantom sample is not sufficient to determine the actual spatial position of the phantom. To achieve this, one must generate signals which may be regarded as projections onto both x and y axes by first applying a gradient, Gx, collecting and transforming the resulting signal and then repeating the process by substituting gradient Gy for Gx as illustrated in Fig.13. One can see, however, from the back projection of these profiles, that an ambiguity remains (Fig.13b). At least one more projection, using for example, a gradient that is tilted 45 degrees, is required to unequivocally determine the location of the samples (Fig.13c). The construction of an image consisting of N x N pixels requires at least N independent views (projections), each defined by N points.

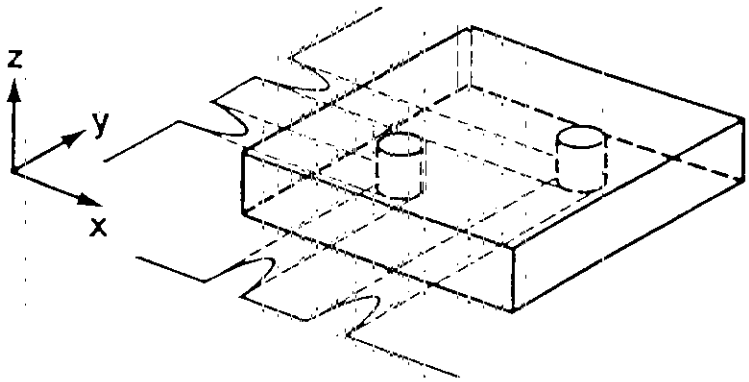

13a. – Projection signals obtained from two water samples situated in the xy plane (x and y projections require signal acquisition in the presence of an x and y gradient, respectively.

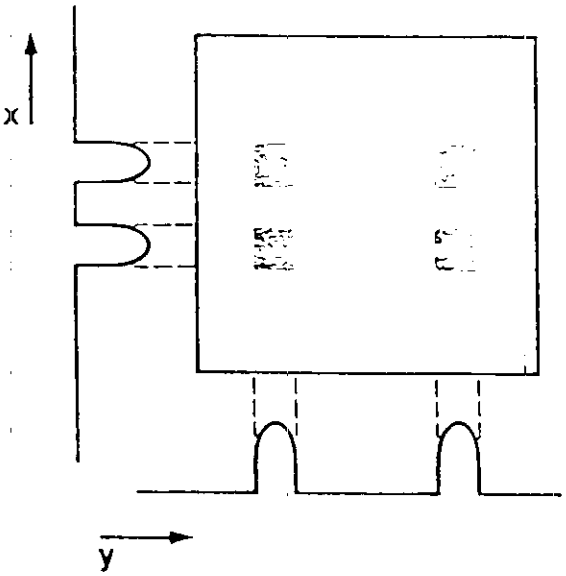

13b. – Principle of image reconstruction by back projection. It is obvious that from two projections, the location of the two samples cannot unequivocally be constructed.

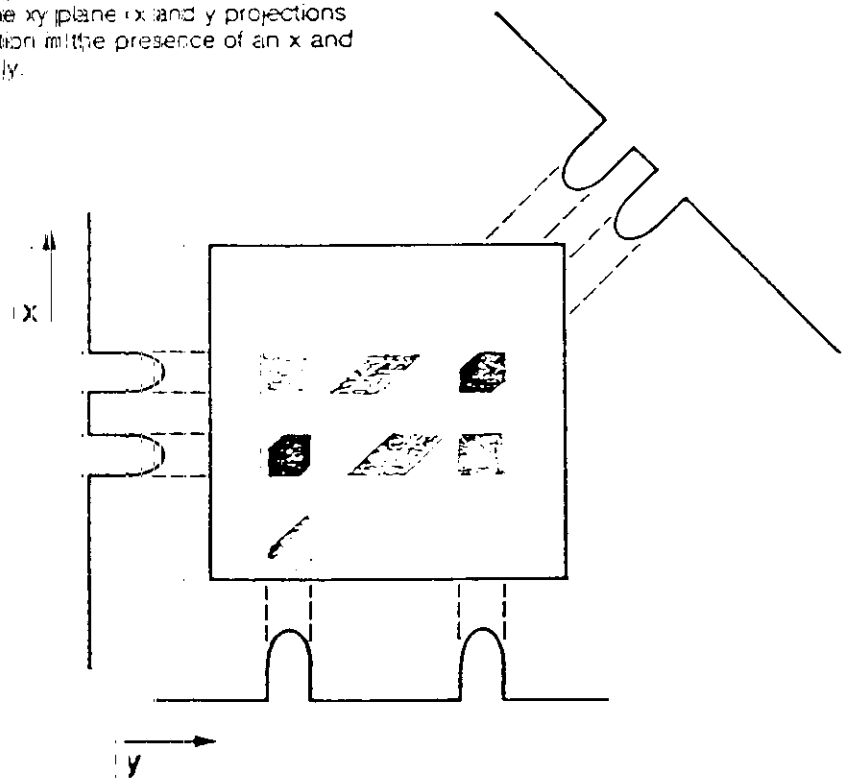

13c. – By back-projecting a third independent profile, the correct coordinates of the two samples can be determined.

Figure 13

The method of image reconstruction by back-projection as demonstrated on Fig. 13 is analogous to x-ray CT, where the attenuation profiles take the place of the NMR frequency-domain signal: Fourier transforms of the phantom free induction decay (measured at 32 different orientations of the phantom with respect to the static magnetic field gradient) are measured and the x-z cross section of the phantom sample is calculated in the IBM PC computer using the standard backprojection reconstruction technique. The resulting MR image is shown on the figure 14. The blur, resulting from simple back-projection, is eliminated by first convolving the projection signals with suitable filter functions, a procedure again well known from x-ray CT.

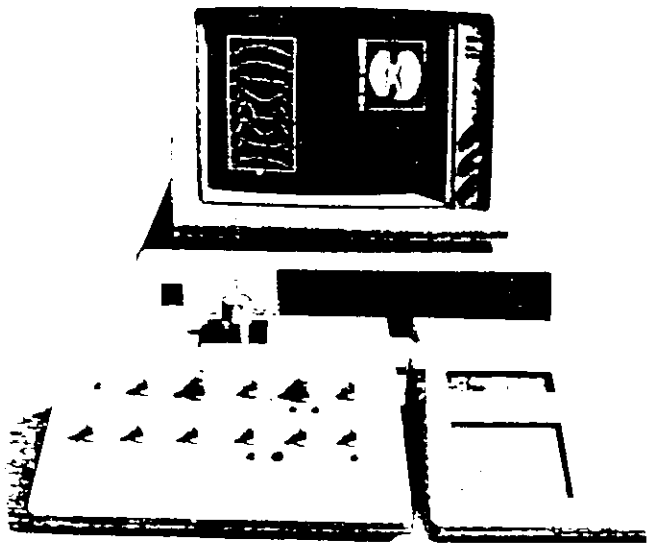

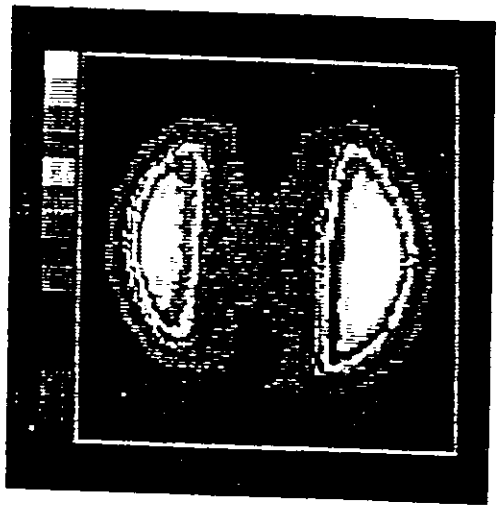

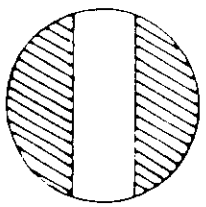

Phantom sample

Figure 14.

Algebraic Reconstruction is iterative reconstruction technique for determining density matrix of protons from projections. It was suggested for use in X-ray tomography (Herman 1973, 1976). It gives significantly better results as simple backprojection technique:

First step of calculation is to determine initial values for the density matrix (n x m). One of the approaches is to start with average density ($\overline{\rho_0}$)

$$\overline{\rho_0}(x,y) = \frac{\sum_{x=1}^{n}\sum_{y=1}^{n}\rho(x,y)}{n^2}$$

Zeroth approximation is then iterated by the following formula

$$\rho_{k+1}(x,y) = \rho_k(x,y) + \frac{P_i(r,\theta) - R_i(r,\theta)}{N_i(r,\theta)},$$

where $P_i(r,\theta)$ is measured value of density (projection data), which is going through point (x,y) at angle θ and $R_i(r,\theta)$ is calculated sum of the elements of the density matrix which go through point (x,y) at angle θ. $N_i(r,\theta)$ is the number of elements that are lying at the angle θ along $R_i(r,\theta)$ in density matrix. One iteration is comprised of the calculation iteration formula for all points in each projection and for all projections (Fig.15).

In principle one should repeat iterative procedure until required accuracy is achieved. This approach could lead to noneffective large number of iterations and long computation time. A.R.T. algorithm converges only when the projection data is accurate. In case of noisy data there is a great chance that the result would diverge. The stability of the iterative procedure can be improved if the corrective factor $s_i<1$ is used. The factor s_i being less than 1 causes the calculated correction not to be completely performed, which means that the result is updated for less than it was estimated to be necessary.

$$\rho_{k+1}(x,y) = \rho_k(x,y) + \delta_i \cdot \frac{P_i(r,\theta) - R_i(r,\theta)}{N_i(r,\theta)}$$

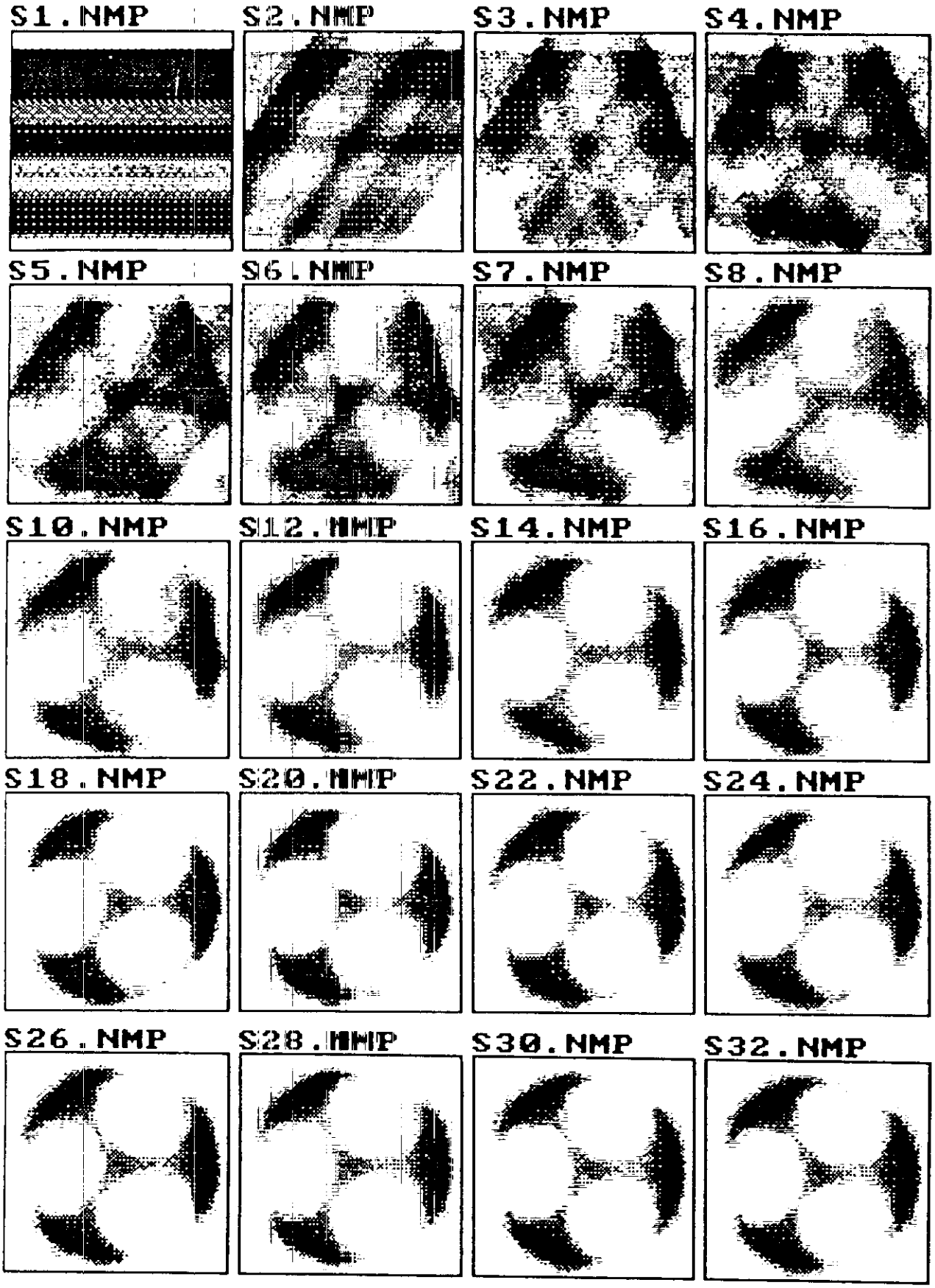

Figure 15. - Gallery of images obtained after consecutive angular dependence measurement (32 steps from 0° to 360° rotation). After the 32's measurement (single rotation for 360°)) the MR Image already represents a very realistic image of the phantom sample.

To remain on the safe side, the value of s≤0.5 is recomended for the first iteration ard value of s≤0.25 for all the others. With the normal quality of the NMR signals a single A.R.T. iteration is sufficient as demonstrated on fig. 16 showing a "gallery" of MR Images of different phantom samples.

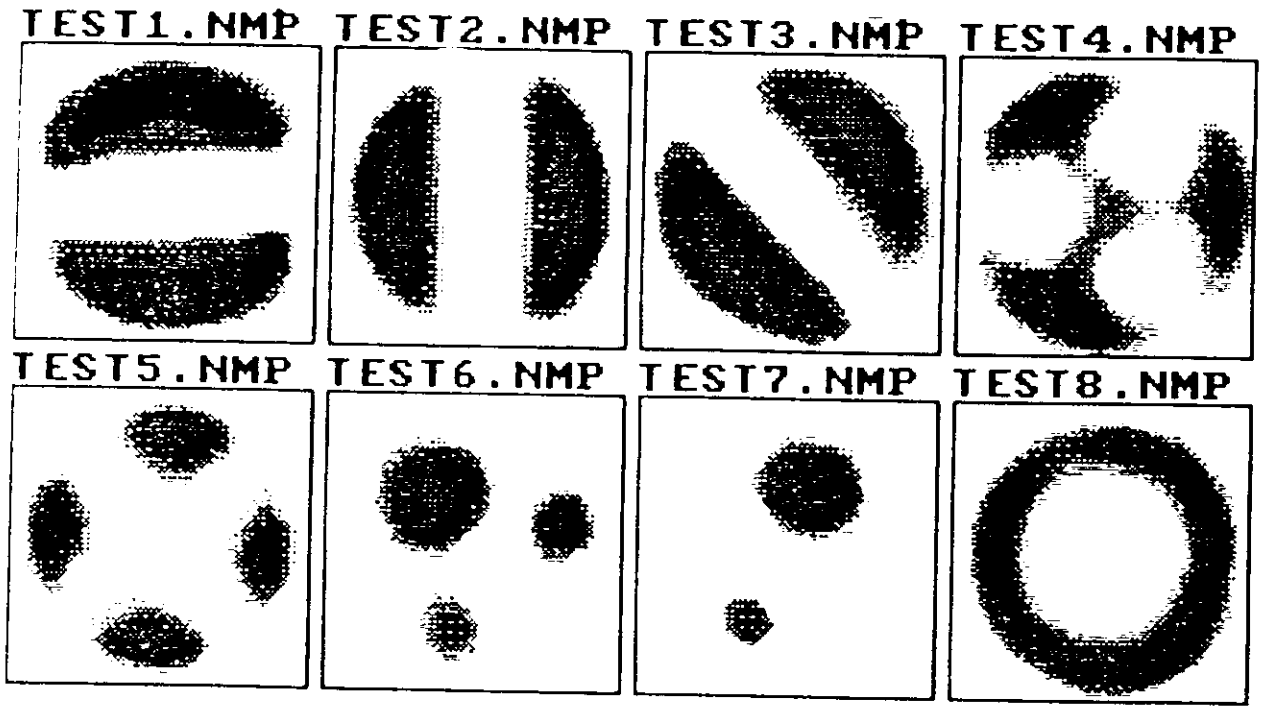

Figure 16. - MR Image gallery: display of MR images of different phantom samples

There are of course many other approaches to the problem of MR imaging and image reconstruction. Most of them make use of timed rather than stationary gradients. Such methods however require a more complex gradient coil system design and would be relatively difficult to demonstrate them in a small permanent magnet built in the SMRI instrument. Nevertheless the simple, one gradient axis, backprojection and A.R.T. technique realized in the IJS Small MR Imager & NMR Spectrometer demonstrate clearly enough what the MR imaging is all about.

Combining the presence of the linear gradient of the z component of the magnetic field with a r.f. pulse that is sufficiently weak and has small frequency bandwidth so, that it can excite only a narrow slice of a thickness z, a cross-sectional images can be obtained (Fig. 17).

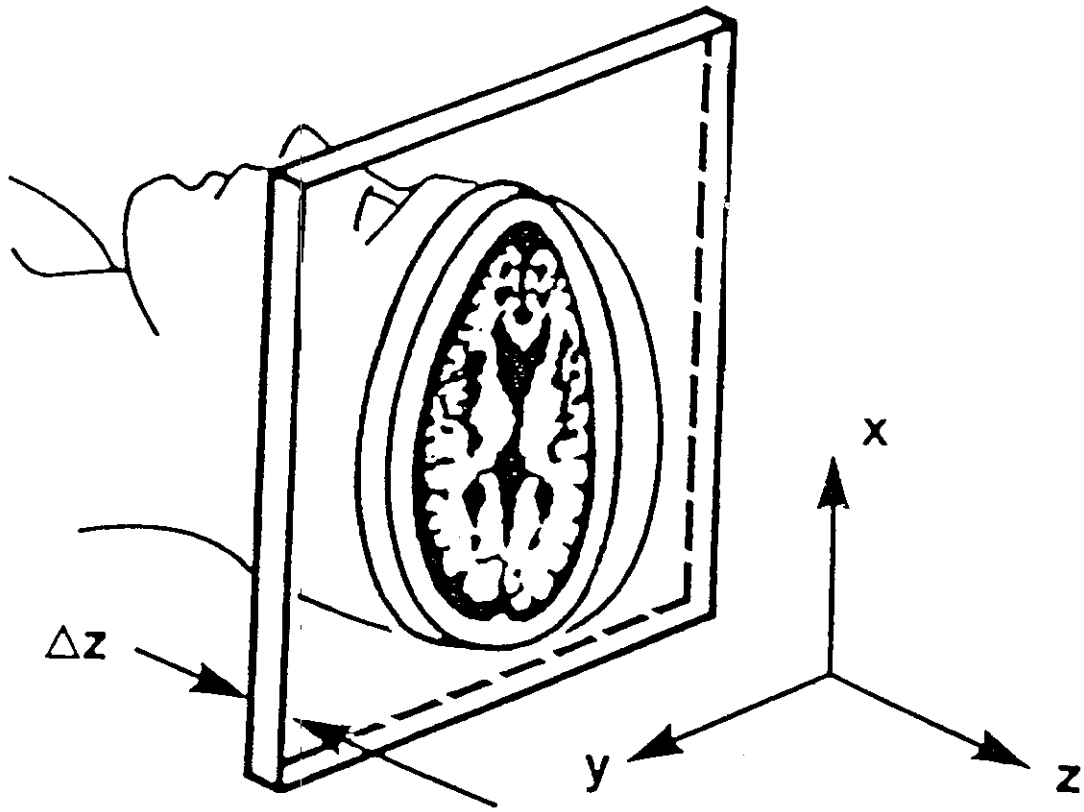

By combining a frequency-selective pulse in the presence of a z gradient, excitation can be confined to a slice of thickness Δz.

Figure 17.